S.T. Yau High School Science Award

Research Report

The Team

Name of team member: Jingshu Wang
School: Suffield Academy
City, Country: Suffield, USA

Name of supervising teacher: Heng Song
Job Title: Professor
School/Institution: Wuhan University
City, Country: Wuhan, China

Title of Research Report

Engineered Probiotic Outer Membrane Vesicles Overcome Therapeutic Barriers in Inflammatory Bowel Disease: An Innovative Strategy Based on Dual-Gene Editing and a ClyA-SOD Membrane Fusion System

Date

July 27, 2026

Engineered Probiotic Outer Membrane Vesicles Overcome Therapeutic Barriers in Inflammatory Bowel Disease: An Innovative Strategy Based on Dual-Gene Editing and a ClyA-SOD Membrane Fusion System

Abstract

Inflammatory bowel disease (IBD), comprising Crohn's disease and ulcerative colitis, is a chronic gastrointestinal disorder with rising global incidence and regional disparities, driven by genetic and environmental factors. Pathogenesis is driven by a vicious cycle of oxidative stress and inflammation, mediated by intestinal barrier dysfunction, reactive oxygen species (ROS) accumulation, and pro-inflammatory cytokine (e.g., TNF-α, IL-6) overproduction. Current therapies face limitations, including systemic toxicity, poor mucosal targeting, and suboptimal bioavailability. Herein, we engineered outer membrane vesicles (OMVs) from *Escherichia coli* Nissle 1917 (EcN) via CRISPR-Cas9-mediated dual knockout of nlpI and degP, enhancing OMV production through metabolic reprogramming and stress-response activation. A ClyA-SOD fusion system enabled directional anchoring of functional superoxide dismutase (SOD) onto OMV surfaces for targeted ROS scavenging. *In vitro*, SOD-OMVs demonstrated superior superoxide anion clearance efficiency compared to free SOD. In a DSS-induced murine IBD model, SOD-OMVs derived from EcN-ΔnlpIΔdegP/ClyA-SOD significantly attenuated colitis progression, outperforming single-gene modified strains and conventional antioxidants. This genetically optimized OMV platform disrupts the IBD inflammatory-oxidative cycle with enhanced precision and biocompatibility, offering a promising nanotherapeutic paradigm for IBD management.

Keywords: Inflammatory Bowel Disease (IBD), Superoxide dismutase (SOD), CRISPR-Cas9 gene editing, Escherichia coli Nissle 1917(EcN), outer membrane vesicles(OMVs)

Table of Contents

1. Introduction……..…5
2. Methods……....8

2.1 Construction of Knockout Cassette Plasmids……8

2.2 Construction of pTarget-sgRNA Plasmids…….……9

2.3 Construction of Gene Knockout Strains……..10

2.3.1 CRISPR-Cas9-Mediated Gene Knockout……...…..10

2.3.2 Verification of Gene Knockout……...……..11

2.3.3 Plasmid Curing……...…11

2.4 Verification of OMV Secretion and ClyA Engineering in EcN…….…..12

2.4.1 Bacterial Culture…….…..12

2.4.2 OMV Isolation……..12

2.4.3 OMV Characterization……..12

2.5 Therapeutic Application of SOD-Loaded OMVs in IBD Treatment……...12

2.5.1 Bacterial Culture……...….12

2.5.2 OMV Isolation……..12

2.5.3 Functional Validation……13

2.6 IBD Mice Model Experiments…….13

2.6.1 Animal Ethics Statement……...13

2.6.2 Preparation of Bacterial Strains and Reagents……...…13

2.6.3 Quantitative Analysis of Mouse IL-6 and TNF-α in IBD Models……14

2.6.4 Hematoxylin and Eosin (H&E) Staining of Murine Colonic Tissues……...15

3. Results……...….15

3.1 Successful Knockout of nlpI and degP Genes in EcN…….15

3.2 Evaluation of the Increase of OMVs from Engineered EcN Strains……...18

3.3 In vitro Superoxide Scavenging Activity of Engineered OMVs…….21

3.4 In vivo Anti-IBD therapy of OMVs from Engineered EcN Strains…….22

4. Discussion……..24
5. Conclusion…….....25
6. References…….25

7. Acknowledgement……..……29
8. Declaration of Academic Integrity……..30

Introduction

Inflammatory bowel disease (IBD) is a group of disorders marked by chronic, recurrent inflammation of the gastrointestinal tract. IBD includes two classical subtypes: Crohn's disease (CD) and ulcerative colitis (UC).[1-3] The most recent Global Burden of Disease (GBD 2021) data shows that the incidence of IBD has consistently increased globally since 1990, with an age-standardized incidence rate of 4.45 cases per 100,000 population, representing an increase from 4.22 cases per 100,000 population in 1990.[4-5] IBD shows by significant regional variation, with a persistent upward trajectory observed across diverse geographic regions and time periods. Notably, North America and Europe exhibit the highest incidence and prevalence rates of IBD, with certain regions showing continued escalation.[6-7] Emerging economies, particularly China, are experiencing rapidly increasing IBD incidence rates, a trend that may be potentially attributable to evolving lifestyle patterns, environmental exposures, and enhanced healthcare accessibility.[8] This distinct difference highlights the combined impact of environmental and genetic factors on disease prevalence and the epidemiology of the disease.[9-10] The essential pathogenesis of IBD is a vicious cycle of inflammation and oxidative stress.[10-12] The disruption of the intestinal mucosal barrier leads to irregular exposure of pathogen-associated molecular patterns (PAMPs) and damage-associated molecular patterns (DAMPs), which activates innate immune cells and triggers excessive production of reactive oxygen species (ROS).[10-11, 13] These oxidative stress products intensify the intestinal inflammation through two important ways. They directly induce oxidative modifications of lipids, proteins, and DNA, thereby causing tissue injury. They also act as secondary messengers to trigger the pro-inflammatory signaling pathways such as NF-κB and MAPK.[10-12] Such signaling pathways causes the excessive production of pro-inflammatory cytokines, including tumor necrosis factor-alpha (TNF-α) and IL-6.[10-12] This increase further disrupts the tight junctions of the intestinal epithelium, causing damage such as degradation of occludin and ZO-1 proteins.[10, 12-13] As a result, the mucosal permeability of the gastrointestinal tract increases, starting a self-reinforcing vicious cycle of oxidative injury, immune activation, and barrier breakdown.[10-11, 13] The continued interaction of inflammatory signals and oxidative stress eventually leads to gut microbiome imbalances, aberrant immune responses in the mucosa, and fibrotic changes, all of which underpin the chronic course of IBD.[12, 14]

Despite advancements in clinical management, the current conventional treatment options used for IBD face multiple bottlenecks. For example, even though biologics like anti-TNF-α monoclonal antibodies can inhibit key inflammatory pathways, they are also associated with risks of systemic immunosuppression and serious infections, while their local delivery efficiency and bioavailability in intestinal mucosal lesions remain limited.[15] Similarly, traditional antioxidants, such as N-acetylcysteine, lack tissue specificity and require high doses to achieve therapeutic concentrations in the gut.[16-17] It also results in adverse events including hepatic and renal toxicity in a significant proportion of cases.[18-19] Although therapeutic innovations such as JAK inhibitors and S1P receptor modulators have partially addressed clinical challenges through mechanistic advancements, suboptimal intestinal drug concentrations and poor mucosal permeability persist as

primary barriers to achieving optimal therapeutic efficacy.[20-21] Therefore , despite the established role of above therapy in IBD management, its clinical application necessitates combination with other therapeutic modalities to optimize therapeutic efficacy and minimize treatment-related adverse events.

Superoxide dismutase (SOD) is an important enzyme in the endogenous antioxidant defense system, playing a key role in neutralizing reactive oxygen species (ROS) such as superoxide anions ($\bullet O_2^-$) to mitigate oxidative stress.[22-23] Animal model studies have demonstrated that SOD can reduce intestinal mucosal damage, though specific percentages of reduction have been reported in some studies.[24] However, the clinical translation of natural SOD is hampered by several challenges. First, oral administration of SOD is limited by rapid degradation by gastric and pancreatic proteases, which can reduce enzymatic activity.[24] Second, intravenous administration of SOD has a short plasma half-life, necessitating frequent dosing and reducing patient compliance.[24-25] Finally, traditional SOD formulations lack targeted delivery to intestinal lesions, with limited bioavailability, severely limiting clinical efficacy .[24-25]

The probiotic *Escherichia coli* Nissle 1917 (EcN) and its outer membrane vesicles (OMVs) present a novel delivery platform for inflammatory bowel disease (IBD) treatment.[26] As a clinically established probiotic with significant therapeutic history, EcN naturally produces OMVs capable of penetrating biological membranes.[27] This inherent property enables efficient traversal across the intestinal mucus barrier and facilitates targeted delivery to intestinal epithelial cells.[28] Notably, EcN's genetic engineering potential allows precise control over therapeutic biomolecule loading in its OMVs.[29-30] Drawing inspiration from EcN research, we propose a parallel strategy using CRISPR-Cas9 to knock out nlpI and degP genes, enhancing OMV production through biosynthetic modulation and stress-induced secretion. NlpI deletion derepresses peptidoglycan hydrolase MepS activity, reprogramming cell wall metabolism to boost OMV production.[31] Concurrent deletion of both nlpI and degP induces accumulation of misfolded periplasmic proteins, activating the Cpx/Rse envelope stress response pathway.[32] This dual-gene knockout creates a synergistic regulatory network exceeding production thresholds achieved by single-gene modifications. Furthermore, leveraging the self-assembly properties of the ClyA membrane protein fusion system[33-34], we aim to construct a superoxide dismutase (SOD)-functionalized OMV platform. This system enables directional anchoring and functional display of SOD on the OMV lipid bilayer. The resulting engineered OMV platform retains EcN's probiotic colonization properties and host compatibility while enabling targeted SOD delivery (Figure 1). This dual-intervention approach could disrupt the inflammatory-oxidative stress cycle in IBD, providing a nanocarrier system with enhanced targeting efficiency and superior biocompatibility.

In this study, we evaluated the therapeutic potential of engineered OMVs derived from EcN for IBD through integrated in vitro and in vivo investigations. CRISPR-Cas9 was employed to generate ΔnlpI, ΔdegP, and dual-knockout EcN variants. The pET28a-ClyA-SOD plasmid was introduced into EcN to enable robust membrane-anchored SOD expression. In vitro analyses confirmed the SOD-OMVs' high-efficiency scavenging capacity for superoxide anions ($\bullet O_2^-$). For

in vivo validation, we utilized a dextran sulfate sodium (DSS)-induced murine IBD model. Therapeutic efficacy was assessed through clinical parameters (weight loss), serum cytokine levels (TNF-α, IL-6), and histopathological evaluation of colonic tissues using the Disease Activity Index (DAI) for barrier integrity assessment Results demonstrated that SOD-OMVs derived from the EcN-ΔnlpIΔdegP/ClyA-SOD strain attenuated colitis progression, outperforming both single-gene modified strains and conventional antioxidant therapies. These findings establish a foundation for developing next-generation IBD therapeutics with enhanced targeting precision and reduced toxicity.

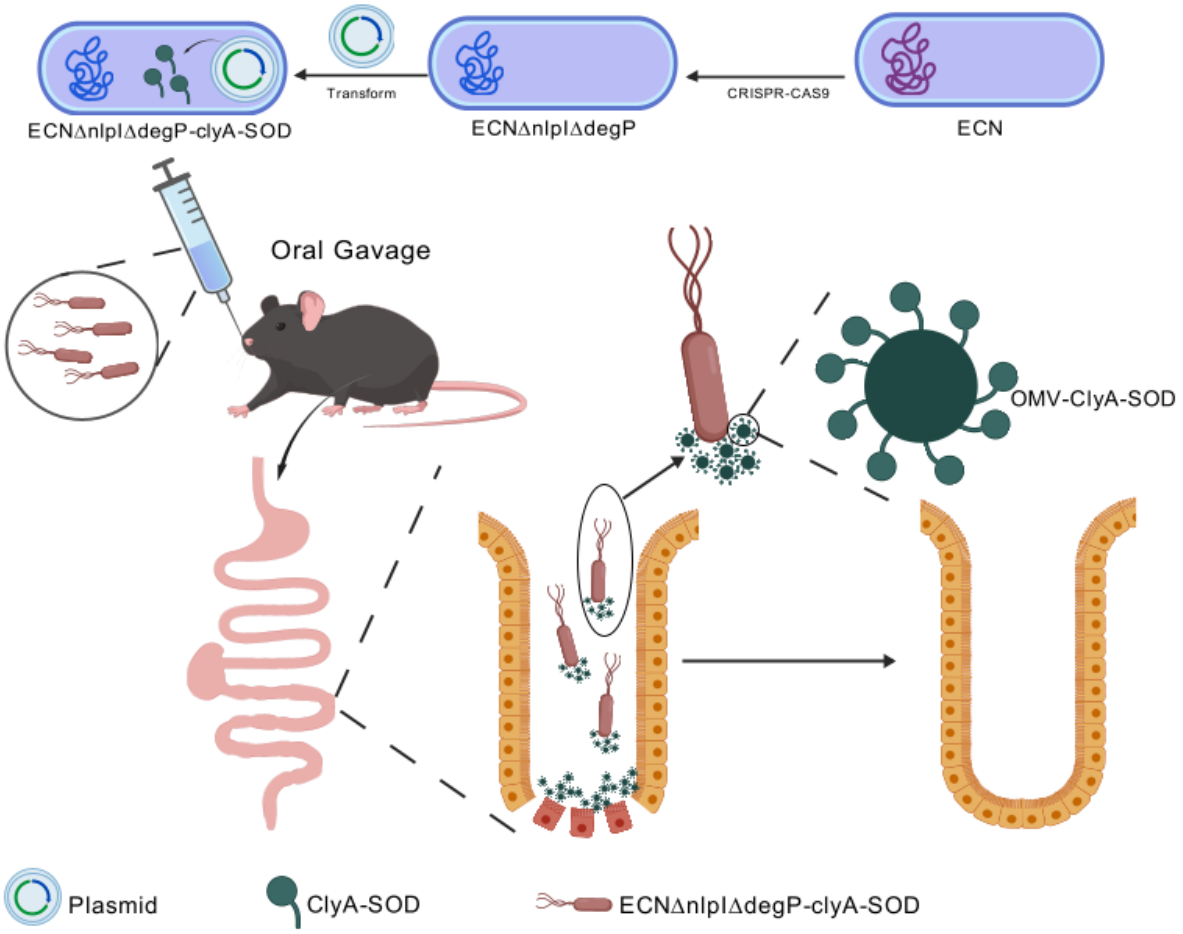


Figure 1. Engineered Probiotics for IBD Treatment. The probiotic EcN was genetically engineered to possess therapeutic effects in relieving IBD. To boost the production of OMVs, the nlpI and degP genes were deleted using CRISPR-Cas9. Additionally, a plasmid expressing SOD was transformed into EcN and SOD was fused to the membrane anchor protein ClyA, allowing its targeted expression within OMVs. The engineered strain, EcNΔnlpIΔdegP-ClyA-SOD, was delivered by oral gavage to mice and shown to be successfully relieving IBD symptoms by efficiently eliminating ROS.

Methods

2.1 Construction of Knockout Cassette Plasmids

To construct CRISPR-Cas9-based gene knockout plasmids targeting *nlpI* and *degP*, we first retrieved the genomic sequence of *Escherichia coli* Nissle 1917 (EcN) from the NCBI GenBank database and imported it into SnapGene software for visualization and design. For each target gene, 500 bp homologous arms (nlpI-arm-up, nlpI-arm-down, degP-arm-up, degP-arm-down) were selected upstream and downstream of the coding region to facilitate homology-directed repair (HDR).

For the *nlpI* knockout construct, the upstream and downstream homologous regions were labeled *nlpI-arm-up* and *nlpI-arm-down*, respectively. Primer pairs were designed as follows:

- *nlpI-up-F*: Forward primer located at the 5′ end of *nlpI-arm-up*
- *nlpI-up-R*: Reverse primer spanning the junction of *nlpI-arm-up* and *nlpI-arm-down*
- *nlpI-down-F*: Forward primer spanning the junction of *nlpI-arm-up* and *nlpI-arm-down*
- *nlpI-down-R*: Reverse primer at the 3′ end of *nlpI-arm-down*

The same strategy was applied to the *degP* gene. The upstream and downstream homologous regions were designated *degP-arm-up* and *degP-arm-down*. Primer design was as follows:

- *degP-up-F*: Forward primer at the 5′ end of *degP-arm-up*
- *degP-up-R*: Reverse primer bridging *degP-arm-up* and *degP-arm-down*
- *degP-down-F*: Forward primer bridging *degP-arm-up* and *degP-arm-down*
- *degP-down-R*: Reverse primer at the 3′ end of *degP-arm-down*
- All primers were designed using SnapGene's primer design tool to ensure optimal Tm, GC content, and minimal secondary structure.

Primer	**Sequence**
nlpI-up-F	TATCGGTAAAGGCGGTTCTGTAATC
nlpI-up-R	GATTACGGGCTGATGTGTACGCATTTCCCACTCCCGAAGAC
nlpI-down-F	GTCTTCGGGAGTGGGAAATGCGTACACATCAGCCCGTAATC
nlpI-down-R	GCGTAATTGCACGTCATAACGT
degP-up-F	CATGTGTTTAGCCATCCAGATGTCGA
degP-up-R	CAGGAAGGGGTTGAGGGAAAGTATTTCAGTCTCGATTAACAGATAAC
degP-down-F	CGTTATCTGTTAATCGAGACTGAAATACTTTCCCTCAACCCCTTCCTG
degP-down-R	AGACCAGTTCGCCATATTTACGCA

Figure 2A: List of Primers.These primers are synthesized construct the knockout cassettes.

Genomic DNA from wild-type *Escherichia coli* Nissle 1917 (EcN) was extracted using the *EasyPure* Genomic DNA Kit according to the manufacturer's protocol. PCR amplification of homologous arms was performed in a 20 μL reaction system containing 7 μL of nuclease-free

water, 1 μL of forward primer (e.g., *nlpI-up-F*), 1 μL of reverse primer (e.g., *nlpI-up-R*), 1 μL of the extracted genomic DNA, and 10 μL of Taq enzyme mix.

The same protocol was applied to amplify the remaining homologous regions: *nlpI-arm-down* (using *nlpI-down-F* and *nlpI-down-R*), *degP-arm-up* (using *degP-up-F* and *degP-up-R*), and *degP-arm-down* (using *degP-down-F* and *degP-down-R*).

All PCR products were verified by agarose gel electrophoresis to confirm the expected fragment sizes prior to cloning.

Gel Extraction of degP Knockout Cassette

Following agarose gel electrophoresis of the PCR product for the degP homologous arms, multiple bands were observed at approximately 500 bp, 1000 bp, and 2000 bp. To isolate the correct 1000 bp degP knockout cassette, the target DNA band was excised under UV light and purified using the US Everbright DNA Gel Extraction Kit according to the manufacturer's protocol. The gel slice was fully dissolved at 75°C in Buffer DE-A, with intermittent mixing to ensure complete liquefaction. Buffer DE-B is added and mixed in. The mixture is then centrifuged several times for 1 min with the speed of 12000g and washed with Buffer W1 and Buffer W2. Eluent was added and after 1 minute in room temperature, the mixture was centrifuged once more and ready for use for downstream applications.

Overlap Extension PCR for Knockout Cassette Assembly

To generate the complete knockout cassette, upstream and downstream homologous arms were fused using overlap extension PCR:

- Reaction mixture (20 μL): 6 μL nuclease-free water, 1 μL forward primer (e.g., *nlpI*-up-F), 1 μL reverse primer (e.g., *nlpI*-down-R), 1 μL *nlpI*-arm-up product, 1 μL *nlpI*-arm-down product, and 10 μL Taq enzyme mix.
- The same method was used for *degP*.

The resulting fused products (*nlpI* and *degP* knockout cassettes) were validated via agarose gel electrophoresis.

2.2 Construction of pTarget-sgRNA Plasmids

To design the single-guide RNA (sgRNA) sequences for *nlpI* and *degP* gene knockouts, we used the CHOPCHOP web tool to identify optimal 20-nucleotide protospacer sequences. These target sequences were incorporated into a pTarget plasmid backbone using SnapGene software by replacing the N20 placeholder region.

For each gene, we designed two primers flanking the protospacer region. The forward primer (e.g., N20-nlpI-F or N20-degP-F) contained the complete 20-nt target sequence and several bases

downstream. The reverse primer (e.g., N20-nlpI-R or N20-degP-R) contained the reverse complement of the 20-nt sequence along with upstream flanking bases. All primers were synthesized by the Genecreate Biological Company, and the pTarget plasmid backbone was obtained from laboratory stocks.

N20-nlpI-F	TGGGATCGCATTATATTACGGGTTTTAGAGCTAGAAATAGCAAGTT
N20-nlpI-R	CCGTAATATAATGCGATCCCACTAGTATTATACCTAGGACTGAGCTAG
N20-degP-F	GGTGCGTTGGTTAACCTGAAGTTTTAGAGCTAGAAATAGCAAGTT
N20-degP-R	TTCAGGTTAACCAACGCACCACTAGTATTATACCTAGGACTGAGCTAG

Site-directed mutagenesis PCR was performed in a 20 μL reaction containing 7 μL nuclease-free water, 1 μL of each primer, 1 μL of the pTarget plasmid template, and 10 μL of Taq polymerase master mix. PCR products were validated via agarose gel electrophoresis.

To eliminate the template pTarget plasmid after PCR, we treated the amplified product with DpnI digestion. Specifically, 2 μL of 10×Buffer Cuts and 0.5 μL of DpnI enzyme were added to the 18 μL of PCR product. The reaction was incubated in a PCR machine. The program was set to 37 °C for 1 hour, followed by 80 °C for 5 minutes.

The reaction mixture was then transformed into chemically competent *E. coli* DH5α cells. Add 79μL of deionized water and 20μL of 5×KCM and 1μL of the plasmid intro competent E.Coli DH5α cells. Then, the mixture was heat shocked at 42°C in a water bath for 90 seconds and immediately transferred to ice for 2 minutes to facilitate transformation. The cells are incubated in 800μL of LB broth at 37°C 1 hour for recovery. Then, the bacterial suspension is centrifuged for 1 minute at 5000rpm. After removing the supernatant, the mixture was cultured on LB agar plates and cultured overnight. Then, the single colonies were inoculated into 1 mL of LB broth containing kanamycin for 8 hours.

Plasmids (pTarget-nlpI and pTarget-degP) were extracted using the AxyPrep Plasmid Miniprep Kit plasmid extraction kit and the plasmids are sent to the GeneCreate Biological Company for screening.

2.3 Construction of Gene Knockout Strains

2.3.1 CRISPR-Cas9-Mediated Gene Knockout

Introduction of Cas9 Plasmid. The Cas9 expression plasmid (pCas9, kanamycin-resistant) was first introduced into wild-type EcN via electroporation. Competent cells were prepared using the 10% glycerol washing method, and 2 ng of pCas9 was electroporated into 100 μL of competent EcN cells. Following electroporation, cells were recovered in 900 μL SOC medium at 37°C, 220 rpm for 1 hour and plated on LB agar supplemented with kanamycin. Verified pCas9-harboring strains were used for subsequent gene knockout experiments.

Preparation of Competent Cells. EcN strains harboring the Cas9 plasmid were cultured on LB agar plates supplemented with kanamycin (50 μg/mL) at 37°C overnight. Single colonies were inoculated into 1 mL of LB broth containing kanamycin and incubated for 3 hours at 37°C, 220

rpm, to obtain seed cultures. Subsequently, 500 µL of seed culture was transferred into 50 mL fresh LB broth and cultured until the optical density at 600 nm (OD_{600}) reached 0.4–0.6 (mid-log phase). Cells were harvested by centrifugation (5000 rpm, 4°C, 5 minutes) and washed three times with ice-cold 10% glycerol. The resulting competent cells were aliquoted into 100 µL portions and stored at –80°C for later use.

Electroporation and Gene Editing. Competent EcN cells were electroporated with 100 ng of pTargetF-nlpI or pTargetF-degP plasmids (carrying spectinomycin resistance) and 400ng of donor DNA containing the nlpI or degP knockout cassettes, depending on the targeted gene. After electroporation, 900 µL SOC recovery medium was added immediately, and cells were incubated at 37°C for 1 hour.

Selection of Positive Transformants. Bacterial cultures were plated onto LB agar containing kanamycin and spectinomycin and incubated overnight at 37°C. Single colonies were picked into 1 mL LB broth containing both antibiotics and cultured for 3–4 hours at 37°C.

Using the method above, we constructed the EcNΔnlpI and EcNΔdegP strains. We repeated the process to the EcNΔnlpI strain and have resulted with the EcNΔnlpIΔdegP

2.3.2 Verification of Gene Knockout

PCR Verification. For each target gene, upstream and downstream primers were designed (nlpI-up-F/R, degP-up-F/R) to validate gene deletion. PCR was conducted in a 20 µL reaction mixture comprising 7 µL nuclease-free water, 1 µL of each primer, 1 µL bacterial suspension, and 10 µL Taq enzyme mix. Successful knockouts were verified by agarose gel electrophoresis, where wild-type strains exhibited a 2000 bp band, while knockout strains displayed a reduced 1000 bp fragment, consistent with the expected deletion size.

2.3.3 Plasmid Curing

Elimination of pTarget Plasmids. To remove pTarget plasmids, bacterial cultures were incubated in LB medium supplemented with 10% L-rhamnose (final concentration), kanamycin, and no spectinomycin for 6 hours at 37°C, 220 rpm.

Dual Antibiotic Screening. Cultures were plated on LB agar plates containing both kanamycin and spectinomycin as well as plates with kanamycin only. Colonies that grew on kanamycin-only plates but failed to grow on dual-antibiotic plates were selected, indicating successful plasmid curing.

Spontaneous Curing of Cas9 Plasmid. Due to the temperature-sensitive origin of replication on the Cas9 plasmid, natural curing occurred during subsequent subcultures without antibiotic selection.

Final Screening of Plasmid-Free Clones. Clones were patched on sucrose plates and LB plates with or without kanamycin. Colonies that failed to grow on kanamycin plates but thrived on antibiotic-free plates were expanded in LB broth and stored for further experiments.

2.4 Verification of OMV Secretion and ClyA Engineering in EcN

2.4.1 Bacterial Culture

Electroporation. Competent cells (100 μL each) of EcN-WT, EcN-ΔnlpIΔdegP, EcN-ΔnlpI, and EcN-ΔdegP were transformed with 200 ng of pET28a-ClyA-eGFP plasmid by electroporation, recovered in 900 μL SOC medium, and incubated at 37°C for 1 hour.

Selection and Induction. Transformed cells were plated on LB agar with kanamycin and incubated overnight. Single colonies were cultured in 1 mL LB with kanamycin at 37°C for 3–4 hours. Cultures were then transferred to 100 mL LB with 50 μg/mL kanamycin, grown at 37°C, 220 rpm, until OD600 reached 0.8–1.0, followed by induction with 1 mM IPTG at 25°C for 20 hours.

2.4.2 OMV Isolation

OMVs were isolated using the bacterial outer membrane vesicle extraction kit (Duolaimi Biotech, Wuhan).

2.4.3 OMV Characterization

- **BCA Assay**: Protein concentration was quantified using the BCA Protein Assay Kit (Biosharp) and a microplate reader.
- **NTA**: OMV particle size and concentration were measured using the ZetaView system (Dulaimi Biotech, Wuhan).
- **Western Blot**: SDS-PAGE was performed followed by transfer to membranes. Detection was done using a His-tag rapid Western blot kit, and bands were visualized with the GelDoc XR+ system (Bio-Rad).

2.5 Therapeutic Application of SOD-Loaded OMVs in IBD Treatment

2.5.1 Bacterial Culture

Electroporation. Competent cells (100 μL each) of EcN-WT, EcN-ΔnlpIΔdegP, EcN-ΔnlpI, and EcN-ΔdegP were electroporated with 200 ng of pET28a-ClyA-SOD plasmid, recovered in 900 μL SOC medium, and incubated at 37°C for 1 hour.

Selection and IPTG Induction. Transformed cells were plated on kanamycin plates, incubated overnight, and cultured in 1 mL LB with kanamycin (37°C, 3–4 hours). Cultures were transferred to 100 mL LB with 50 μg/mL kanamycin, induced with 1 mM IPTG at OD600 of 0.8–1.0, and further incubated at 25°C for 20 hours.

2.5.2 OMV Isolation

OMVs were isolated using the commercial bacterial OMV isolation kit (Duolaimi Biotech, Wuhan).

2.5.3 Functional Validation

Western Blot. OMV protein composition was analyzed using SDS-PAGE and His-tag Western blotting, with visualization by the Bio-Rad GelDoc XR+ imaging system.

In Vitro Activity Assay. The superoxide anion scavenging capacity of OMVs was determined using a commercially available kit (Boxbio, catalog number AKA0025M), following the manufacturer's protocol. Briefly, OMV samples were prepared by ultrasonication (200 W, 3 s on, 10 s off, 30 cycles) on ice, followed by centrifugation at 12,000 × g, 4°C, for 10 minutes. The supernatant was collected for subsequent analysis.

The reaction mixture included sequential addition of five reagents provided in the kit. Each sample reaction and blank control contained 10 μL reagent one, 40 μL reagent two, 25 μL deionized water, and 50 μL each of reagents three, four, and five. After thorough mixing, the samples were incubated at 37°C for designated times (30 min or 20 min), and absorbance was recorded at 530 nm using a microplate reader.

The superoxide scavenging activity was calculated using the following formula:

$$Scavenging\ Rate(\%) = \frac{A_{blank} - A_{sample}}{A_{blank}} \times 100\%$$

All measurements were performed in triplicate.

2.6 IBD Mice Model Experiments

2.6.1 Animal Ethics Statement

All animal experiments were conducted in accordance with the ethical guidelines approved by the Wuhan University Animal Care and Use Committee. Efforts were made to minimize animal suffering, and all procedures complied with national regulations on laboratory animal welfare.

2.6.2 Preparation of Bacterial Strains and Reagents

Preparation of Bacterial Strains for Oral Gavage. Engineered EcN: EcN-SOD, EcN-ΔnlpIΔdegP/SOD, and wild-type EcN streaked onto LB agar plates containing kanamycin (50 μg/mL) and incubated overnight at 37°C. A single colony was inoculated into 1 mL of LB broth with kanamycin and cultured at 37°C, 220 rpm for 3–4 hours to obtain seed cultures. Subsequently, 50 μL of kanamycin stock solution and 500 μL of seed culture were transferred into 50 mL of fresh LB broth and incubated at 37°C with shaking for 1 hour until the OD_{600} was measured. The bacterial cultures were harvested by centrifugation at 8000 rpm for 5 minutes, and the pellets were washed three times with sterile phosphate-buffered saline (PBS). After the final wash, the bacterial suspensions were adjusted to an OD_{600} of approximately 1.0 using PBS. A final volume of 100 μL was prepared per mouse for oral gavage administration. This creates a dosage of 1×10^8 CFU per mouse. The dosage of 1×10^8 CFU per mouse per administration was selected based on prior studies

demonstrating effective colonization and therapeutic effects of EcN strains in murine colitis models.

Preparation of Drinking Water. Acute IBD was induced using dextran sulfate sodium (DSS, molecular weight 36,000–50,000 Da, MP Biomedicals). Mice received 3% (w/v) DSS dissolved in drinking water for a total of 5 days, followed by normal drinking water until sacrifice. IPTG (1 mM final concentration) was continuously supplied in the drinking water throughout the experimental period to induce SOD expression in bacterial strains.

2.6.3 Quantitative Analysis of Mouse IL-6 and TNF-α in IBD Models

ELISA Protocol for Quantitative Mouse IL-6 Detection in IBD Models. Samples including serum, plasma, tissue homogenates, and cell lysates were prepared according to standardized protocols (Amoy lunchangshuo Biotech, IL-6 ELISA KIT). Blood specimens were collected in endotoxin-free tubes, with serum obtained via 2000 ×g centrifugation after 4°C overnight storage. Plasma was derived from EDTA-anticoagulated blood centrifuged within 30 min, while tissues underwent ice-cold PBS washing, mincing, and homogenization (1:9 w/v ratio) with proteinase inhibitors as needed. Cell lysates were generated through freeze-thaw cycles or sonication, followed by clarification at 2000 ×g. All samples were stored at -80°C in single-use aliquots. Reagents were equilibrated to 25°C for ≥1 h prior to use, with wash buffer prepared by diluting concentrated solution 1:20 in distilled water.

The ELISA protocol involved loading 50 μL of standards, diluted samples, or diluent (blank) into pre-coated 96-well strips, followed by 100 μL HRP-conjugated antibody incubation at 37°C for 45 min. Plates were washed 5× with 350 μL buffer per cycle, then incubated with 3,3',5,5'-Tetramethylbenzidine (TMB) substrates (50 μL each) in the dark for 15 min. Reactions were terminated with 50 μL stop solution, and absorbance was measured at 450 nm. Data analysis utilized a 4-parameter logistic curve fit for standard concentrations, with sample concentrations interpolated and adjusted for dilution factors. Statistical evaluation was performed using GraphPad Prism v9.0, adhering to MIQE guidelines for reproducibility.

ELISA Protocol for Quantitative Mouse TNF-α Detection in IBD Models. Biological samples including serum, plasma, tissue homogenates, and cell lysates were processed following standardized protocols (Amoy lunchangshuo Biotech, TNF-α ELISA KIT). Blood was collected in non-endotoxin tubes, with serum obtained via 2000 ×g centrifugation after 4°C overnight storage. Plasma was derived from EDTA-anticoagulated blood centrifuged within 30 min (2000 × g, 15 min). Tissues underwent PBS washing, mincing, and homogenization (1:9 w/v ratio) on ice, followed by sonication or freeze-thaw cycles and clarification at 5000 ×g. Cell lysates were generated from 1×10^6 cells resuspended in 150-200 μL PBS, with lysates clarified at 2000 ×g. All samples were stored at -80°C in aliquots. Reagents were equilibrated to 25°C for 1 h, with wash buffer prepared by diluting 20× concentrate 1:20 in distilled water.

Pre-coated 96-well strips were loaded with 50 μL of standards, diluted samples, or diluent (blank). HRP-conjugated antibody (100 μL) was added to each well, followed by sealing and incubation at 37°C for 45 min. Plates were washed 5× with 350 μL buffer per cycle, then incubated with TMB substrates (50 μL each) at 37°C for 15 min in the dark. Reactions were terminated with

50 μL stop solution, and absorbance was measured at 450 nm within 15 min. Data were analyzed using a 4-parameter logistic curve fit ($R^2 > 0.99$), with sample concentrations interpolated and adjusted for dilution factors. Quality control parameters included assay sensitivity (1.0 pg/mL), specificity (no cross-reactivity), and intra/inter-plate CVs (<10%). Statistical evaluation was performed using GraphPad Prism v9.0.

2.6.4 Haematoxylin and Eosin (H&E) Staining of Murine Colonic tissues.

Tissue Processing and Preservation. Mice were euthanized by cervical dislocation after surface disinfection with 75% ethanol. The colonic segment from the cecal junction to the anus was dissected, and a 0.5 cm distal colonic sample was fixed in 4% paraformaldehyde (PFA) at 4°C for 24 h. The remaining intestinal tissue was flash-frozen in liquid nitrogen and stored at -80°C for molecular analyses.

Paraffin Section Preparation. Freshly dissected colonic tissues were immediately immersed in 4% PFA at room temperature for ≥24 h. Fixed tissues were trimmed with a scalpel under a chemical fume hood, labeled, and placed into embedding cassettes. Tissue dehydration and wax infiltration were performed using an automated tissue processor (Leica ASP300S). Processed tissues were embedded in paraffin wax blocks using a paraffin embedding station (Leica EG1150H). Serial sections (4 μm thickness) were cut using a rotary microtome (Leica RM2255) and floated in a 40°C water bath. Sections were mounted onto glass slides and dried in a 60°C oven for 2 h prior to storage at room temperature.

HE Staining Protocol. Paraffin sections underwent deparaffinization and rehydration through sequential immersion in two changes of environmentally friendly dewaxing solution (20 min each), followed by 100% ethanol (two changes, 5 min each) and 75% ethanol (5 min), with thorough rinsing in distilled water between steps. Sections were pre-treated with HD constant dye pre-treatment solution for 1 min to enhance staining consistency. For hematoxylin staining, slides were incubated in hematoxylin solution for 3-5 min, differentiated in 1% acid alcohol, blued in bluing solution, and rinsed under running water. Eosin counterstaining involved dehydration in 95% ethanol (1 min) prior to 15 s incubation in eosin solution. Dehydration and mounting were performed by clearing sections through graded ethanol (100% ethanol, three changes), n-butanol (two changes), and xylene substitutes (two changes, 2 min each), with neutral balsam applied for coverslip sealing.

Results

3.1 Successful Knockout of nlpI and degP Genes in EcN.

Escherichia coli Nissle 1917 (EcN) is a well-established probiotic strain with a long history of clinical application and safety in human health.[27] To enhance the production of outer membrane

vesicles (OMVs) from EcN, we employed the CRISPR-Cas9 system to target and delete the nlpI and degP genes, which are known to regulate peptidoglycan metabolism and envelope stress responses, respectively.[31-32] Previous studies have demonstrated that the deletion of nlpI relieves the repression of the peptidoglycan endopeptidase MepS, thereby promoting peptidoglycan hydrolysis and enhancing OMV production.[31] The deletion of degP induces the accumulation of misfolded periplasmic proteins, activating the Cpx/Rse envelope stress response pathway. The combined effect of these two genetic modifications is expected to significantly enhance OMV production.[32]

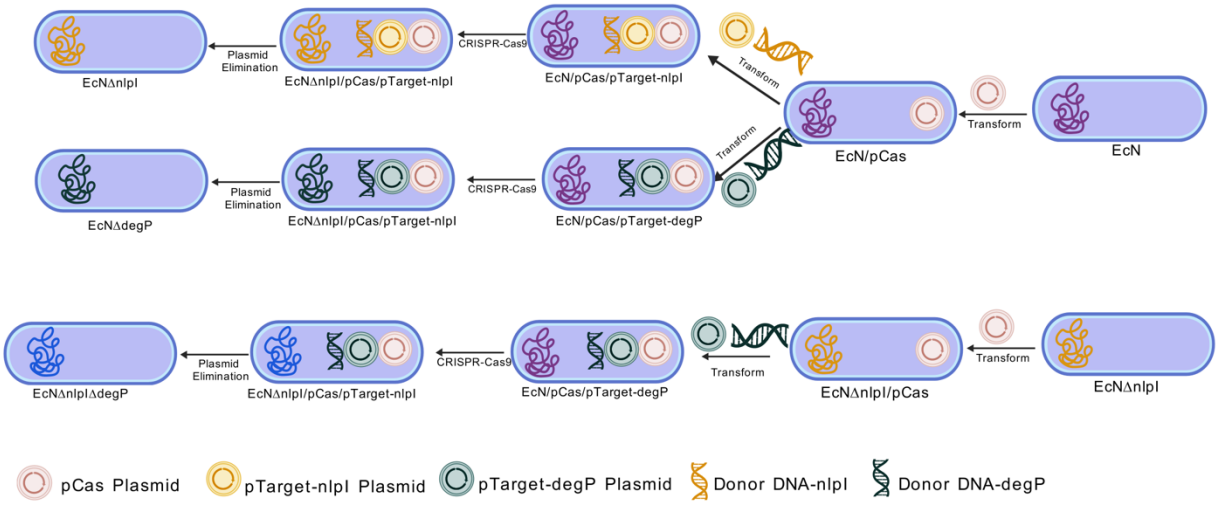


Figure 2. Schematic workflow of CRISPR-Cas9-mediated double-gene knockout in EcN. The pCas9 plasmid (kanamycin-resistant) was first introduced into wild-type EcN via electroporation. For gene targeting, pTargetF plasmids carrying the sgRNA targeting either nlpI or degP (spectinomycin-resistant) and donor DNA carrying the homologous arms were electroporated into pCas9-harboring EcN cells. Plasmid curing was then carried out using L-rhamnose-induced counterselection for pTarget and temperature-sensitive replication for pCas9.

To generate the desired knockout strains, we designed and constructed single-gene knockout strains (EcN-ΔnlpI, EcN-ΔdegP) and a double-knockout strain (EcN-ΔnlpIΔdegP), as shown in Figure 2. The CRISPR-Cas9-mediated gene knockout was performed using homology-directed repair (HDR). The primers and knockout cassettes were designed using SnapGene software (version 2025) . The upstream and downstream regions of the nlpI and degP genes were amplified via PCR and subsequently fused via overlap extension PCR to generate the HDR templates. The success of the amplification and fusion was confirmed by agarose gel electrophoresis, as shown in Figure 3. The resulting knockout cassettes were then used to construct the donor DNA for the CRISPR-Cas9 system.

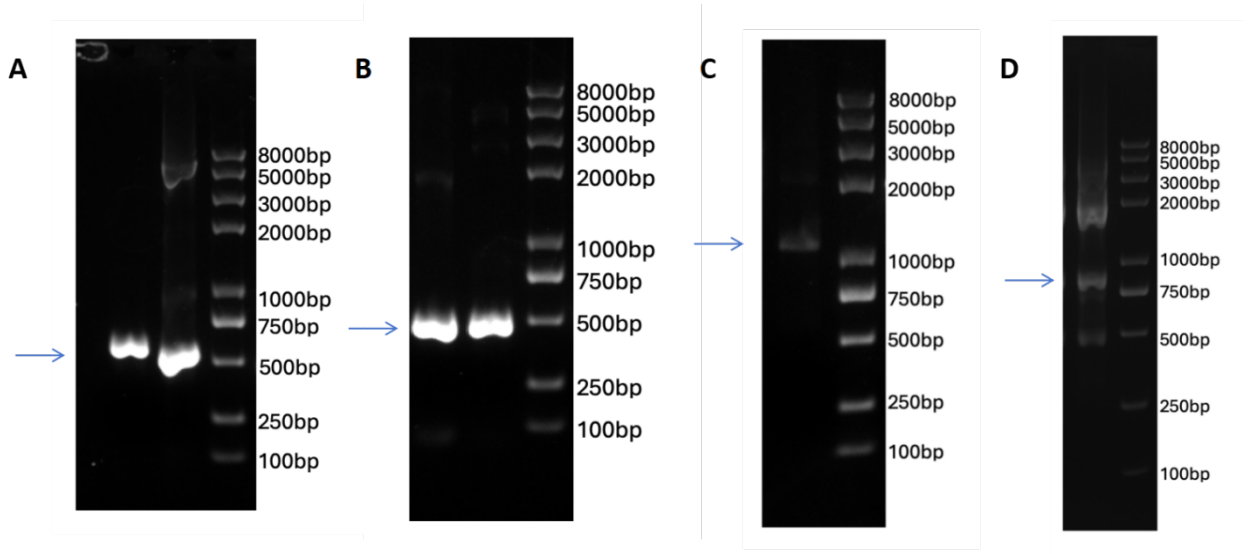


Figure 3. PCR Amplification and Assembly of Homologous Arms for nlpI and degP Genes. Agarose gel electrophoresis was used to verify the amplification and assembly of homologous arms and knockout cassettes. The results demonstrate successful PCR amplification of the nlpI and degP homologous arms (A and B), as well as the assembly of nlpI and degP knockout cassettes (C and D). The gel electrophoresis confirms the expected sizes of the PCR products, with DNA markers included for size reference. For the degP knockout cassette (D), assembled by overlap extension PCR, a major band at approximately 1000 bp corresponds to the expected size of the full-length degP knockout cassette. Additional non-specific bands at approximately 500 bp and 2000 bp may indicate partial or incomplete fusion. To isolate the correct construct, the ~1000 bp band was excised and purified using a gel extraction kit for downstream applications.

To construct the pTarget plasmid containing the sgRNA targeting nlpI and degP for the CRISPR-Cas9 knockout, the CHOPCHOP website[35] is used to identify 20-nt protospacer sequences and incorporated them into the pTarget backbone via site-directed mutagenesis PCR. Primers containing the target sequences were designed and used to replace the N20 region of the plasmid. Agarose gel electrophoresis was used to verify the success of the PCR (Figure 4A and 4B). After PCR amplification, the original template plasmid was digested with DpnI to ensure specificity. The resulting constructs were transformed into E. coli DH5α, and successful plasmids were extracted for downstream applications.

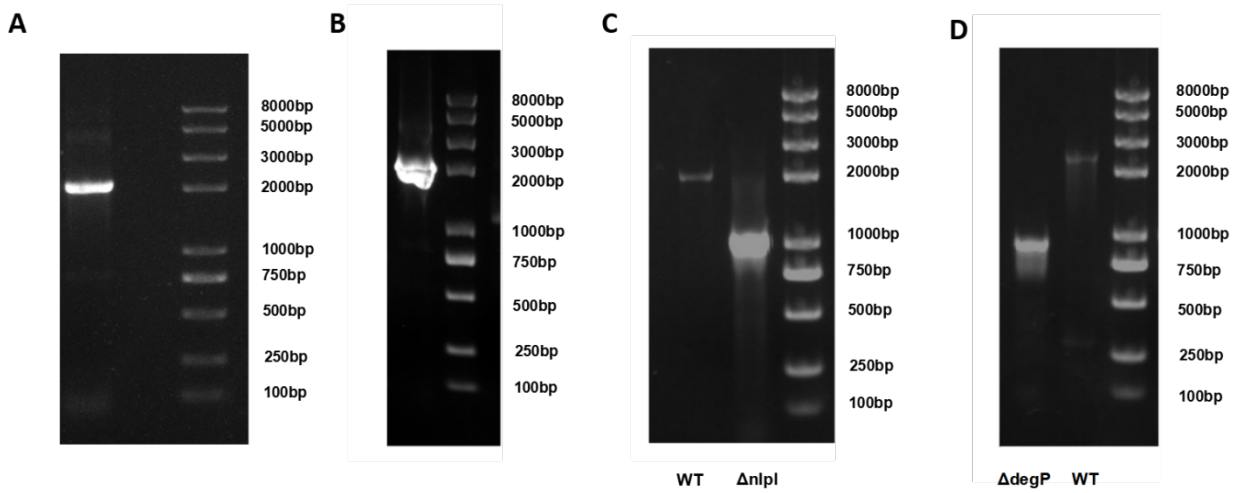


Figure 4. PCR Amplification and Gel Electrophoresis Verification of Plasmid and Gene Knockout. Agarose gel electrophoresis was used to verify the successful amplification and knockout of specific genes and plasmids.(A) and (B) The successful amplification of the pTarget-nlpI and pTarget-degP plasmids, respectively. Both fragments display clear bands at approximately 2000 bp, confirming the expected sizes of the PCR products. (C) and (D) show the verification of gene knockout using CRISPR-Cas9-mediated editing. In Figure 4C, the wild-type EcN strain (left) shows a band at ~2000 bp, while the ΔnlpI mutant (right) shows a smaller band at ~1000 bp, confirming successful deletion of the nlpI gene. (D) The wild-type EcN strain (right) shows a band at ~2000 bp, while the ΔdegP mutant (left) shows a smaller band at ~1000 bp, confirming successful deletion of the degP gene. A DNA marker is included for size reference.

We evaluated the efficiency of gene editing by PCR amplification followed by agarose gel electrophoresis (Figure 4C and 4D). Specific primers were designed to amplify the target gene regions: in the wild-type strain, both nlpI and degP produced amplicons of approximately 2000 bp, whereas in the knockout strains, homologous recombination resulted in the deletion of key gene fragments, reducing the expected product size to approximately 1000 bp. The results of the gel electrophoresis demonstrated that all engineered strains displayed distinct bands at 1000 bp, in sharp contrast to the 2000 bp bands observed in the wild-type control group. This distinct reduction in band size (Δbp = 1000 bp) confirmed the successful knockout of the target genes, consistent with the theoretical expectations of homologous recombination-mediated gene editing. Based on the aforementioned approaches described above, we engineered EcN using CRISPR-Cas9 gene editing technology, yielding single-gene knockout strains (EcN-ΔnlpI, EcN-ΔdegP) and a double-knockout strain (EcN-ΔnlpIΔdegP). These engineered strains provided a foundational platform for subsequent experiments in this study.

3.2 Evaluation of the Increase of OMVs from Engineered EcN Strains

ClyA is a pore-forming toxin produced by *Escherichia coli* and related bacteria, which naturally integrates into bacterial outer membranes and forms pore structures in OMVs.[33-34] To validate the

efficacy of our OMVs-based delivery platform, we first constructed a fusion gene encoding enhanced green fluorescent protein (eGFP) and ClyA, using eGFP as a reporter. This fusion construct was subsequently introduced into the aforementioned engineered ECN strains. Upon expression, the eGFP moiety co-localizes with ClyA in the OMVs of these engineered bacteria. By isolating OMVs from different ECN strains and quantifying eGFP content, we can assess variations in OMV secretion capacity among the engineered strains. This approach allows identification of the optimal ECN strain with superior OMV production capability. Subsequent replacement of the eGFP gene with therapeutic protein-encoding sequences would enable utilization of ECN-derived OMVs for delivery of therapeutic proteins, thereby establishing a foundation for translational applications in health treatment.

The impact of genetic modifications on outer membrane vesicle (OMV) bioproduction in EcN was evaluated using the bicinchoninic acid (BCA) protein assay. This colorimetric method quantifies protein concentration through Cu^{2+} reduction and formation of a purple-colored complex (λ = 562 nm). OMV yields were compared across four engineered strains: wild-type (EcN-WT/ClyA-eGFP), single-gene knockouts (EcN-ΔnlpI/ClyA-eGFP and EcN-ΔdegP/ClyA-eGFP), and a double-knockout strain (EcN-ΔnlpI/ΔdegP/ClyA-eGFP). Following ultracentrifugation-based purification (100,000×g, 4°C, 2 h), BCA analysis (Fig. 5) revealed significant interstrain variation in OMV production.

Baseline OMV protein concentration in the wild-type control was 154 μg/mL. Relative to this reference, single-gene knockout strains demonstrated enhanced production: 3.11-fold increase in ΔnlpI and 2.98-fold increase in ΔdegP strains. Notably, the double-knockout variant (EcN-ΔnlpI/ΔdegP) exhibited a 4.36-fold production increase compared to wild-type, surpassing yields observed in single-knockout counterparts. This indicates independent enhancement effects from nlpI and degP deletion, with dual-knockout demonstrating synergistic amplification beyond additive expectations.

The observed enhancement patterns may suggest potential underlying mechanisms: nlpI deletion could relieve MepS inhibition, potentially accelerating peptidoglycan turnover, while degP deletion might activate components of the Cpx/Rse envelope stress response system. The supra-additive effect observed in the double-knockout strain suggests a possible synergistic interaction between these pathways, overcoming inherent limitations of single-gene modifications. While further mechanistic studies are required to confirm these hypotheses, the observed phenotypic outcomes present a promising strategy for optimizing OMV-based bioproduction systems through genetic engineering approaches.

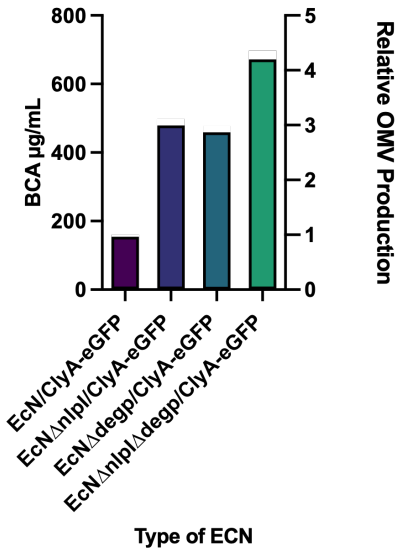


Figure 5. BCA protein quantification of OMVs derived from engineered EcN strains. The total protein concentration of OMVs was measured using the BCA assay. OMVs from the ΔnlpIΔdegP strain exhibited a significantly higher protein content—approximately 4.36-fold greater than that of wild-type EcN—indicating enhanced OMV production following dual-gene knockout.

Nanoparticle tracking analysis (NTA) was then employed to quantitatively assess OMV production across the engineered strains (Fig. 6). This technique enables simultaneous determination of particle size distribution (50–200 nm) and concentration through laser scattering-based tracking of Brownian motion trajectories. Baseline OMV concentration in wild-type EcN (EcN-WT/ClyA-eGFP) was measured at 2.1×10^{10} particles/mL. Single-gene knockout strains demonstrated marked elevation in OMV production, with concentrations reaching 5.4×10^{10} particles/mL (ΔnlpI) and 5.3×10^{10} particles/mL (ΔdegP). Notably, the double-knockout strain (EcN-ΔnlpI/ΔdegP/ClyA-eGFP) exhibited a supra-additive response, achieving 1.2×10^{11} particles/mL - a 5.7-fold increase relative to wild-type that surpassed both single-knockout concentrations and the theoretical additive threshold (5.35-fold).

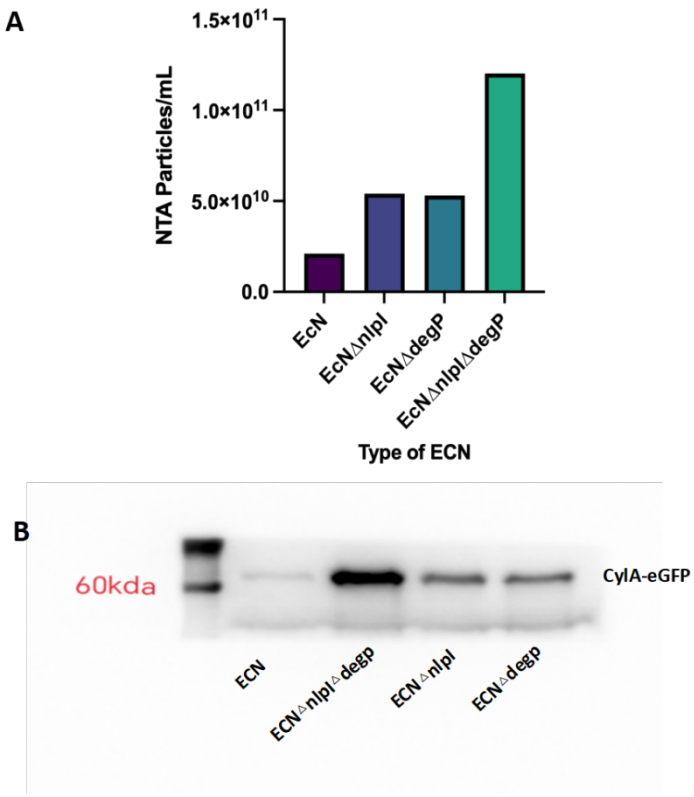


Figure 6. Results of nanoparticle tracking analysis (A) and western blot analysis (B) of OMVs from engineered EcN strains. NTA revealed that OMVs derived from the double-knockout ΔnlpIΔdegP strain exhibited a higher particle concentration compared to wild-type EcN, confirming that dual-gene knockout promotes increased OMV secretion. Western blotting confirmed the successful expression and OMV loading of the ClyA-eGFP fusion protein.

Western blot analysis was performed using anti-eGFP antibodies (target CylA-eGFP protein size ~65 kDa) to confirm and quantify the loading efficiency of the reporter protein into outer membrane vesicles (OMVs). Equal total protein loading was ensured across all samples. As shown in Fig. 6B, OMVs isolated from the EcN-ΔnlpI/ΔdegP/ClyA-eGFP strain exhibited significantly elevated eGFP signals compared to both single-gene knockout strains (ΔnlpI and ΔdegP) and the wild-type control. These cumulative findings demonstrate that while individual nlpI or degP deletion substantially enhances OMV biogenesis, their combined deletion creates a synergistic effect exceeding simple additive contributions. This dual-knockout strategy represents a superior approach for optimizing OMV production systems through genetic engineering.

3.3 *In vitro* Superoxide Scavenging Activity of Engineered OMVs

To assess therapeutic potential, the double-knockout strain EcN-ΔnlpI/ΔdegP (exhibiting maximal OMV production) was selected for superoxide dismutase (SOD) loading. OMVs derived from EcN-ΔnlpI/ΔdegP were isolated and analyzed via western blot using anti-SOD antibodies to

confirm protein expression and vesicular localization (Fig. 7A). SOD detection in OMV fractions validated successful encapsulation and retention of functional enzyme.

The ROS-scavenging capacity of engineered SOD-OMVs was evaluated using a commercial superoxide anion ($\cdot O_2^-$) scavenging assay kit (Boxbio). Absorbance measurements at 530 nm were conducted per manufacturer protocols to quantify scavenging efficiency. OMVs derived from EcN-ΔnlpI/ΔdegP-ClyA-SOD demonstrated significant $\cdot O_2^-$ sequestration (43.1% efficiency), representing a approximately two-fold increase compared to control OMVs.

These findings confirm tha SOD maintains enzymatic activity when encapsulated in engineered OMVs. The observed scavenging efficiency provides *in vitro* validation for the therapeutic potential of these OMVs, supporting their application in subsequent murine models of inflammatory bowel disease (IBD).

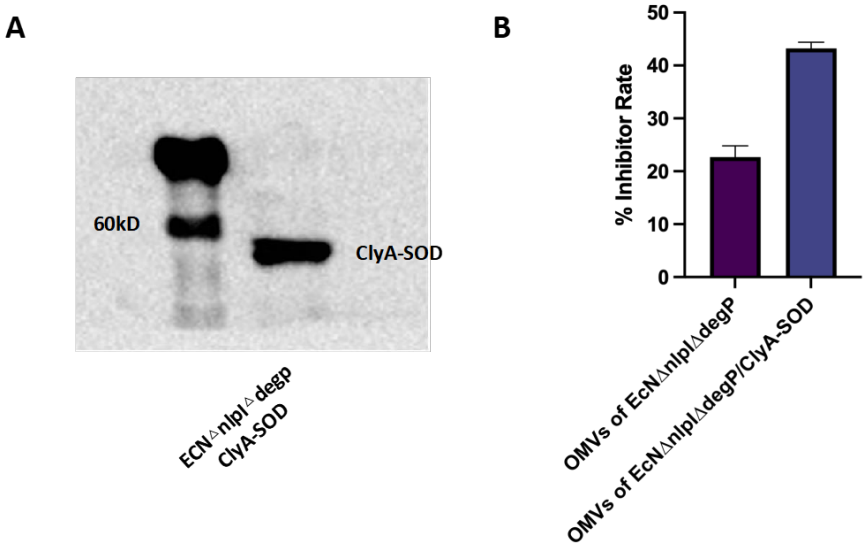


Figure 7. Western blot analysis confirming SOD expression in OMVs derived from EcN-ΔnlpIΔdegP-ClyA-SOD (A) and *in vitro* superoxide anion scavenging activity of engineered OMVs (B). The superoxide scavenging capacity of OMVs derived from EcN-ΔnlpIΔdegP-ClyA-SOD was evaluated using a superoxide anion detection kit. Compared to control OMVs, EcNΔnlpIΔdegP-ClyA-SOD OMVs showed significantly enhanced scavenging of $\cdot O_2^-$, indicating successful functional expression of SOD and its antioxidant activity in vitro.

3.4 *In vivo* Anti-IBD therapy of OMVs from Engineered EcN Strains

Given the observed scavenging efficiency provided *in vitro* validation for the therapeutic potential of these OMVs, their therapeutic potential and application in inflammatory bowel disease (IBD) was assessed in dextran sulfate sodium (DSS) induced acute IBD mice model. Twenty male C57BL/6 mice (6-8 weeks old) were randomly assigned to five experimental groups (n=4 per group) and acclimated for 3 days prior to interventions (Figure 8a). Group 1 (Healthy Control)

received standard diet without dextran sulfate sodium (DSS) treatment. Groups 2-5 underwent colitis induction via ad libitum access to 3% (w/v) DSS-supplemented drinking water for 5 days. Administration protocols were standardized across experimental groups (Groups 2-5) for whole 7 days, with all cohorts receiving oral gavage (0.1 mL formulations) every other day containing either phosphate-buffered saline (PBS) or engineered EcN strains at 1×10^8 colony-forming units (CFU) per dose. Specifically, Group 2 received PBS alone, Group 3 received wild-type EcN, Group 4 received SOD-expressing EcN, and Group 5 received dual-gene knockout EcN (ΔnlpI/ΔdegP) expressing SOD. This experimental design enabled comparative analysis of OMV-based antioxidant delivery in IBD models.

In comparison to the DSS + PBS control group, mice administered with genetically engineered EcN (ΔnlpI/ΔdegP/ClyA-SOD) exhibited significantly reduced serum concentrations of IL-6 (56.85 ± 7.16 pg/mL) and TNF-α (294.43 ± 52.24 pg/mL) as shown in Fig. 8A. Notably, TNF-α levels in the treated group were even lower than those measured in the healthy control cohort (305.14 ± 66.40 pg/mL), while IL-6 concentrations approached physiological levels (55.40 ± 9.06 pg/mL). In colonic tissue, TNF-α levels demonstrated a similar trend, with the EcN(SOD)-treated group showing significantly lower concentrations (328.30 ± 56.45 pg/mL) compared to both DSS + PBS controls and wild-type EcN-treated mice. These findings indicate that SOD expression through OMV delivery contributes to partial amelioration of IBD symptoms. However, suboptimal OMV production in this engineered strain prevented complete resolution of pathological manifestations.

Haematoxylin and eosin (H&E) staining of murine colonic tissues revealed distinct histopathological differences among experimental groups (Fig. 8C and 8D). In the PBS-treated cohort, colonic architecture remained largely intact, characterized by abundant intestinal glands in the lamina propria, well-preserved goblet cell populations, and an unbroken mucosal epithelial layer with no significant infiltration of inflammatory cells. Conversely, DSS-induced colitis in the PBS + 3% DSS group demonstrated marked pathological alterations, including focal mucosal epithelial denudation, partial loss of crypt architecture, and reduced goblet cell density. Notably, mice administered with EcN (ΔnlpI/ΔdegP/ClyA-SOD) exhibited histopathological features comparable to the PBS control group, with partial reversal of DSS-induced damage and significantly reduced histopathological scores (Fig. 8C). In contrast, therapeutic intervention with EcN or EcN(SOD) failed to ameliorate colonic pathology, as these groups displayed histopathological profiles similar to the DSS-treated cohort with persistent mucosal abnormalities and elevated histopathological scores. Collectively, our results demonstrate that dual gene knockout (nlpI/degP) combined with SOD-expressing OMV delivery significantly potentiates OMV-mediated therapeutic efficacy against IBD. These observations highlight the potential of engineered probiotics for targeted inflammatory modulation, though further optimization of OMV yield is required to achieve full clinical efficacy.

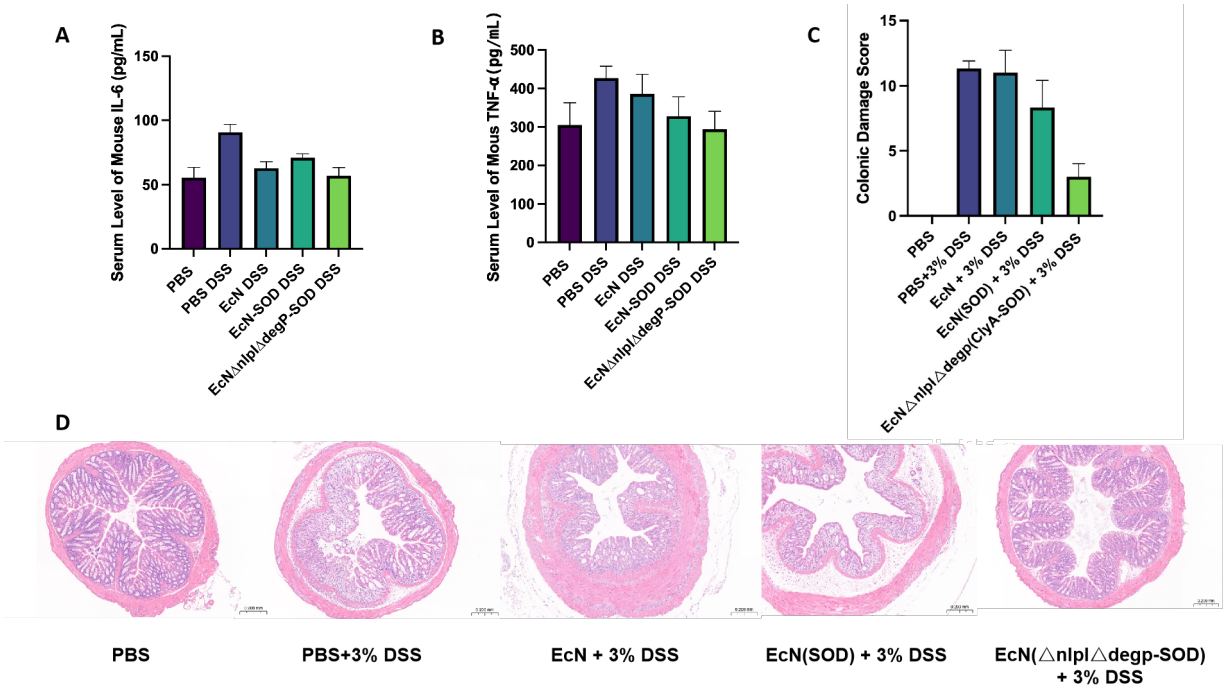


Figure 8. *In vivo* anti-IBD therapy of OMVs from Engineered EcN Strains. (A) and (B) Serum IL-6 and TNF-α levels in murine colitis models treated with engineered EcN strains. A: Quantitative analysis of serum IL-6 and TNF-α concentrations measured by ELISA in mice from different experimental groups. (C) Colon Injury Score Distribution in Experimental Groups. (D) Histological image of murine colonic tissues after H&E staining.Error bars indicated means ± SD (n=3).

Discussion

In this study, we successfully engineered EcN strains with single or double deletions of nlpI and degP genes using CRISPR-Cas9 technology, achieving a significant enhancement in OMV production. The double-knockout strain (EcN-ΔnlpIΔdegP) demonstrated a 4.36-fold increase in OMV protein yield and a 5.7-fold elevation in particle concentration compared to wild-type EcN, as quantified by BCA assay and NTA. These findings align with prior reports that nlpI deletion relieves peptidoglycan hydrolysis inhibition via MepS activation, while degP deletion induces envelope stress responses, collectively amplifying OMV biogenesis. Notably, the synergistic effect observed in the double-knockout strain exceeds simple additive contributions, suggesting interconnected regulatory pathways that warrant further mechanistic exploration.

The therapeutic potential of engineered OMVs was validated through *in vitro* superoxide scavenging assays and in vivo murine models of inflammatory bowel disease (IBD). OMVs derived from EcN-ΔnlpIΔdegP expressing SOD exhibited a 43.1% scavenging efficiency for superoxide anions, outperforming control OMVs. In DSS-induced colitis, these SOD-loaded OMVs significantly reduced serum and colonic levels of pro-inflammatory cytokines (IL-6, TNF-

α) and ameliorated histopathological damage, with efficacy surpassing wild-type EcN or single-knockout variants. However, while histopathological scores improved, complete resolution of IBD symptoms was not achieved, likely due to suboptimal OMV dosage or transient delivery kinetics. Future optimization of OMV yield, stability, and targeted delivery could enhance therapeutic outcomes.

This study advances previous work by demonstrating that dual genetic modulation of peptidoglycan metabolism and envelope stress pathways provides a superior strategy for OMV enhancement compared to single-gene modifications. The use of EcN, a clinically validated probiotic, further underscores the translational potential of this platform. Limitations include reliance on an acute IBD model, which may not fully replicate chronic human pathology, and the absence of long-term safety or immunogenicity assessments. Additionally, while SOD activity was preserved in OMVs, the encapsulation efficiency and biodistribution of therapeutic proteins require systematic optimization.

Conclusion

This study establishes a CRISPR-Cas9-based genetic engineering platform for EcN that significantly enhances OMV production through dual deletion of nlpI and degP. The resulting OMVs demonstrate robust *in vitro* antioxidant activity and *in vivo* anti-inflammatory efficacy in a murine IBD model, highlighting their potential as a protein delivery system for gastrointestinal diseases. By combining probiotic safety with engineered OMV functionality, this approach offers a scalable and biocompatible alternative to synthetic nanocarriers. Future work will focus on optimizing OMV production scalability, evaluating chronic disease models, and exploring therapeutic cargo diversification to broaden clinical applications.

Reference

1. Molodecky NA, Soon IS, Rabi DM, Ghali WA, Ferris M, Chernoff G, Benchimol EI, Panaccione R, Ghosh S, Barkema HW, Kaplan GG. Increasing incidence and prevalence of the inflammatory bowel diseases with time, based on systematic review. *Gastroenterology* 2012; 142: 46-54.e42.

2. Dignass A, Van Assche G, Lindsay JO, Lémann M, Söderholm J, Colombel JF, Danese S, D'Hoore A, Gassull M, Gomollón F, Hommes DW, Michetti P, O'Morain C, Oresland T, Windsor A, Stange EF, Travis SP. The second European evidence-based Consensus on the diagnosis and management of Crohn's disease: Current management. *J Crohns Colitis* 2010; 4: 28-62.

3. Dignass A, Lindsay JO, Sturm A, Windsor A, Colombel JF, Allez M, D'Haens G, D'Hoore A, Mantzaris G, Novacek G, Oresland T, Reinisch W, Sans M, Stange E, Vermeire S, Travis S, Van Assche G. Second European evidence-based consensus on the diagnosis and management of ulcerative colitis part 2: current management. *J Crohns Colitis* 2012; 6: 991-1030.

4. Lin D, Jin Y, Shao X, Xu Y, Ma G, Jiang Y, Xu Y, Jiang Y, Hu D. Global, regional, and national burden of inflammatory bowel disease, 1990-2021: Insights from the global burden of disease 2021. *Int J Colorectal Dis.* 2024 Sep 7;39(1):139.

5. Chen L, Xu Y, Ai F, Shen S, Luo Y, Li X. Dissecting the rising tide of inflammatory bowel disease among youth in a changing world: insights from GBD 2021. *Int J Colorectal Dis.* 2025 Feb 18;40(1):44.

6. Mak WY, Zhao M, Ng SC, Burisch J. The epidemiology of inflammatory bowel disease: East meets west. *J Gastroenterol Hepatol.* 2020 Mar;35(3):380-389.

7. Molodecky NA, Soon IS, Rabi DM, Ghali WA, Ferris M, Chernoff G, Benchimol EI, Panaccione R, Ghosh S, Barkema HW, Kaplan GG. Increasing incidence and prevalence of the inflammatory bowel diseases with time, based on systematic review. *Gastroenterology*. 2012 Jan;142(1):46-54.e42.

8. Hracs L, Windsor JW, Gorospe J, Cummings M, Coward S, Buie MJ, Quan J, Goddard Q, Caplan L, Markovinović A, Williamson T, Abbey Y, Abdullah M, Abreu MT, Ahuja V, Raja Ali RA, Altuwaijri M, Balderramo D, Banerjee R, Benchimol EI, Bernstein CN, Brunet-Mas E, Burisch J, Chong VH, Dotan I, Dutta U, El Ouali S, Forbes A, Forss A, Gearry R, Dao VH, Hartono JL, Hilmi I, Hodges P, Jones GR, Juliao-Baños F, Kaibullayeva J, Kelly P, Kobayashi T, Kotze PG, Lakatos PL, Lees CW, Limsrivilai J, Lo B, Loftus EV Jr, Ludvigsson JF, Mak JWY, Miao Y, Ng KK, Okabayashi S, Olén O, Panaccione R, Paudel MS, Quaresma AB, Rubin DT, Simadibrata M, Sun Y, Suzuki H, Toro M, Turner D, Iade B, Wei SC, Yamamoto-Furusho JK, Yang SK, Ng SC, Kaplan GG; Global IBD Visualization of Epidemiology Studies in the 21st Century (GIVES-21) Research Group. Global evolution of inflammatory bowel disease across epidemiologic stages. *Nature*. 2025 Jun;642(8067):458-466.

9. Corridoni D, Arseneau KO, Cominelli F. Inflammatory bowel disease. *Immunol Lett.* 2014 Oct;161(2):231-5.

10. Gyires K, Tóth ÉV, Zádori SZ. Gut inflammation: current update on pathophysiology, molecular mechanism and pharmacological treatment modalities. *Curr Pharm Des.* 2014;20(7):1063-81.

11. Tian T, Wang Z, Zhang J. Pathomechanisms of Oxidative Stress in Inflammatory Bowel Disease and Potential Antioxidant Therapies. *Oxid Med Cell Longev.* 2017;2017:4535194.

12. Cao SS. Cellular Stress Responses and Gut Microbiota in Inflammatory Bowel Disease. *Gastroenterol Res Pract*. 2018 Jun 20;2018:7192646.

13. Hu C, Liao S, Lv L, Li C, Mei Z. Intestinal Immune Imbalance is an Alarm in the Development of IBD. *Mediators Inflamm.* 2023 Jul 31;2023:1073984.

14. Zhang Y, Chu X, Wang L, Yang H. Global patterns in the epidemiology, cancer risk, and surgical implications of inflammatory bowel disease. *Gastroenterol Rep (Oxf).* 2024 Jul 9;12:goae053.

15. D'Haens GR, van Deventer S. 25 years of anti-TNF treatment for inflammatory bowel disease: lessons from the past and a look to the future. *Gut.* 2021 Jul;70(7):1396-1405.

16. Aruoma OI, Halliwell B, Hoey BM, Butler J. The antioxidant action of N-acetylcysteine: its reaction with hydrogen peroxide, hydroxyl radical, superoxide, and hypochlorous acid. *Free Radic Biol Med.* 1989;6(6):593-7.

17. Samuni Y, Goldstein S, Dean OM, Berk M. The chemistry and biological activities of N-acetylcysteine. *Biochim Biophys Acta.* 2013 Aug;1830(8):4117-29.

18. Aboubakr HM, Elzohairy EA, Ali AA, Rashed LA, Elkady NK, Soliman AS. Therapeutic effects of N-acetylcysteine against malathion-induced hepatotoxicity. *Egypt J Forensic Sci* 2019; 9:34-42..

19. Park WY. Controversies in acetaminophen nephrotoxicity. *Kidney Res Clin Pract.* 2020 Mar 31;39(1):4-6.

20. Roskoski R Jr. Janus kinase (JAK) inhibitors in the treatment of inflammatory and neoplastic diseases. *Pharmacol Res.* 2016 Sep;111:784-803.

21. Juif PE, Kraehenbuehl S, Dingemanse J. Clinical pharmacology, efficacy, and safety aspects of sphingosine-1-phosphate receptor modulators. *Expert Opin Drug Metab Toxicol.* 2016 Aug;12(8):879-95.

22. Islam MN, Rauf A, Fahad FI, Emran TB, Mitra S, Olatunde A, Shariati MA, Rebezov M, Rengasamy KRR, Mubarak MS. Superoxide dismutase: an updated review on its health benefits and industrial applications. *Crit Rev Food Sci Nutr.* 2022;62(26):7282-7300.

23. Rasheed Z. Superoxide dismutase: Challenges, opportunities, and promises for clinical translation. *Int J Health Sci (Qassim)*. 2024 May-Jun;18(3):1-3.

24. Schilrreff P, Simioni YR, Jerez HE, Caimi AT, de Farias MA, Villares Portugal R, Romero EL, Morilla MJ. Superoxide dismutase in nanoarchaeosomes for targeted delivery to inflammatory macrophages. *Colloids Surf B Biointerfaces.* 2019 Jul 1;179:479-487.

25. Borgstahl GEO, Oberley-Deegan RE. Superoxide Dismutases (SODs) and SOD Mimetics. *Antioxidants (Basel)*. 2018 Nov 2;7(11):156.

26. Chen Y, Wan Z, Li ZJ. Development of Sucrose-Utilizing *Escherichia coli* Nissle 1917 for Efficient Heparosan Biosynthesis. *Metabolites.* 2025 Jun 18;15(6):410.

27. Hu R, Lin H, Li J, Zhao Y, Wang M, Sun X, Min Y, Gao Y, Yang M. Probiotic *Escherichia coli* Nissle 1917-derived outer membrane vesicles enhance immunomodulation and antimicrobial activity in RAW264.7 macrophages. *BMC Microbiol.* 2020 Aug 27;20(1):268.

28. Guo S, Chen S, Ma J, Ma Y, Zhu J, Ma Y, Liu Y, Wang P, Pan Y. *Escherichia coli* Nissle 1917 Protects Intestinal Barrier Function by Inhibiting NF-κB-Mediated Activation of the MLCK-P-MLC Signaling Pathway. *Mediators Inflamm.* 2019 Jul 3;2019:5796491.

29. Chen H, Lei P, Ji H, Yang Q, Peng B, Ma J, Fang Y, Qu L, Li H, Wu W, Jin L, Sun D. Advances in *Escherichia coli* Nissle 1917 as a customizable drug delivery system for disease treatment and diagnosis strategies. *Mater Today Bio*. 2023 Jan 6;18:100543.

30. Fang M, Zhang R, Wang C, Liu Z, Fei M, Tang B, Yang H, Sun D. Engineering probiotic *Escherichia coli* Nissle 1917 to block transfer of multiple antibiotic resistance genes by exploiting a type I CRISPR-Cas system. *Appl Environ Microbiol.* 2024 Oct 23;90(10):e0081124.

31. Aktar S, Okamoto Y, Ueno S, Tahara YO, Imaizumi M, Shintani M, Miyata M, Futamata H, Nojiri H, Tashiro Y. Incorporation of Plasmid DNA Into Bacterial Membrane Vesicles by Peptidoglycan Defects in *Escherichia coli*. *Front Microbiol.* 2021 Nov 29;12:747606.

32. Ojima Y, Yamaguchi K, Taya M. Quantitative Evaluation of Recombinant Protein Packaged into Outer Membrane Vesicles of *Escherichia coli* Cells. *Biotechnol Prog.* 2018 Jan;34(1):51-57.

33. Liu H, Song P, Zhang H, Zhou F, Ji N, Wang M, Zhou G, Han R, Liu X, Weng W, Tan H, Wang S, Zheng L, Jing Y, Su J. Synthetic biology-based bacterial extracellular vesicles displaying BMP-2 and CXCR4 to ameliorate osteoporosis. *J Extracell Vesicles.* 2024 Apr;13(4):e12429.

34. Sepahdar Z, Miroliaei M, Bouzari S, Khalaj V, Salimi M. Surface Engineering of *Escherichia coli*-Derived OMVs as Promising Nano-Carriers to Target EGFR-Overexpressing Breast Cancer Cells. *Front Pharmacol.* 2021 Nov 18;12:719289.

35. Labun K, Montague TG, Krause M, Torres Cleuren YN, Tjeldnes H, Valen E. CHOPCHOP v3: expanding the CRISPR web toolbox beyond genome editing. *Nucleic Acids Res.* 2019 Jul 2;47(W1):W171-W174.

Acknowledgment

I want to express my gratitude to Prof. Heng Song, my mentor, who gave me insightful comments on my data analysis as well as crucial recommendations throughout my project. Additionally, I want to thank Yinyin Feng, who assisted me by offering important counsel on the required experiments. Lastly, I want to express my gratitude to Wuhan University for providing me with the chance to study molecular biology in their lab.

Declaration of Academic Integrity

The participating team declares that the paper submitted is comprised of original research and results obtained under the guidance of the instructor. To the team's best knowledge, the paper does not contain research results, published or not, from a person who is not a team member, except for the content listed in the references and the acknowledgment. If there is any misinformation, we are willing to take all the related responsibilities.

Name of team members: Jingshu Wang

Signatures of team members

Name of the instructor: Heng Song

Signature of the instructor: 

Date: July 27, 2026